IOPscience iopscience.iop.org

Home Search Collections Journals About Contact us My IOPscience

Atomistic simulation of a 60° shuffle dislocation segment migrating in a Ge/SiGe(001) epitaxial film

This article has been downloaded from IOPscience. Please scroll down to see the full text article.

2005 J. Phys.: Condens. Matter 17 7505

(http://iopscience.iop.org/0953-8984/17/48/004)

View the table of contents for this issue, or go to the journal homepage for more

Download details:
IP Address: 129.252.86.83
The article was downloaded on 28/05/2010 at 06:52

Please note that terms and conditions apply.

INSTITUTE OF PHYSICS PUBLISHING JOURNAL OF PHYSICS: CONDENSED MATTER
J. Phys.: Condens. Matter **17** (2005) 7505–7515 doi:10.1088/0953-8984/17/48/004

Atomistic simulation of a 60° shuffle dislocation segment migrating in a Ge/SiGe(001) epitaxial film

A Marzegalli, F Montalenti and Leo Miglio

INFM and L-NESS, Dipartimento di Scienza dei Materiali, Università degli Studi di Milano-Bicocca, Via Cozzi 53, I-20125 Milano, Italy

E-mail: leo.miglio@unimib.it

Received 1 July 2005, in final form 20 October 2005
Published 11 November 2005
Online at stacks.iop.org/JPhysCM/17/7505

Abstract
We show that the migration process of a 60° shuffle dislocation in an heteroepitaxial $Ge/Si_{0.5}Ge_{0.5}(001)$ system can be analysed by classical molecular dynamics simulations. By following the misfit segment during its motion, we build a sequence of strain maps giving detailed information about the elastic-energy relaxation in the film. The atomic-scale mechanisms underlying the dislocation motion towards the interface are also monitored, showing, for instance, that kinks are actually present along the dislocation line.

(Some figures in this article are in colour only in the electronic version)

1. Introduction

Heteroepitaxial systems based on SiGe films on Si(001) are particularly important for recent microelectronic applications, and the way that the strain originated by the misfit in the lattice parameters is released via the occurrence of a misfit dislocation network in the film is a critical issue [1, 2]. In a simple thermodynamic model proposed by Matthews [3] a critical film thickness h_c, depending on misfit, is predicted for the nucleation of dislocations in a coherent heteroepitaxial film, when the elastic energy produced by the tetragonal distortion of the film lattice equals the one originated by the dislocation, including the misfit reduction obtained by removing one atomic plane in the film (see also [4, 5]). Actually, the control of such a process, preserving the structural quality of the film, is experimentally difficult, and computer-simulated predictions of the nucleation and migration modalities of dislocations would be rather helpful. Still, the study of realistic situations is hindered by the large size of the system (h_c spans between 100 and 1000 Å for Ge content between 25% and 2.5% [6]) and by the exceedingly long times for dislocation nucleation and migration. Otherwise very interesting results, concerning in particular dislocation migration, are already provided for different systems, such as bulk iron (see [7]).

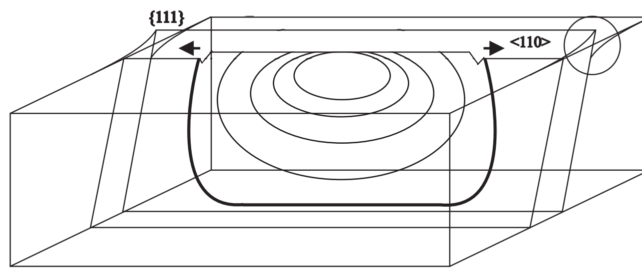

Figure 1. Dislocations nucleate as circular loops. Threading arms tend to repel each other, while the misfit segment migrates towards the interface.

By selecting sufficiently large lattice misfits, i.e. large Ge contents in the film, h_c can actually be reduced to such an extent that the system represented by a critical SiGe film on a Si substrate with a free surface can be simulated by classical potential molecular dynamics, for the high dislocation density produced by periodic boundary conditions in the two dimensions. However, the timescale for activated processes, such as nucleation and migration of dislocations, is still outside the range of molecular dynamics methods.

In order to overcome such an issue, we propose here the following strategy. First, an atomistic dislocation segment is created in the simulation cell, close to the surface, by applying a macroscopic displacement pattern corresponding to the Burgers vector and the set of a 60° dislocation, so that the actual core and the strain distribution are obtained by molecular dynamics simulations. In particular, a shuffle set can be created so that, due to the very small activation energy for misfit segment migration towards the interface (as promoted by a sizeable misfit stress), the microscopic motion of the dislocation core and the related strain field can be followed by additional molecular dynamics runs at a suitable temperature.

In the following we will detail our method and outline our first results for the case of the $Ge/Si_{0.5}Ge_{0.5}(001)$ heteroepitaxial system, which is elastically equivalent to the $Si_{0.5}Ge_{0.5}/Si(001)$ case, still allowing for an atomistic analysis of the strain evolution in the Ge film, with no superposition of the elastic effects created by the compositional disorder.

2. Description of the system and simulation procedure

The most popular dislocations in heteroepitaxial films with the diamond structure are the 60° ones, where the angle corresponds to the one formed by the Burgers vector ($\vec{b}$) and the dislocation line. Therefore, it corresponds to a mixture of pure edge (90°) and pure screw (0°) dislocations. Due to its strong edge component, such extended defects allow for a significant strain relaxation in the growth plane. At the same time, these dislocations are able to migrate towards the substrate, progressively relaxing the film, regardless of where they have nucleated [1, 2].

In real heteroepitaxy, 60° dislocations generally nucleate as loops close to the surface: the dislocation line is initially circular. Due to the strain field, loops increase their radius by moving along a given *glide* $\{111\}$ plane, until they reach the free surface. At this point, the loop becomes semicircular. As is sketched in figure 1, further evolution driven by the strain field involves the formation of an almost linear misfit segment, and two threading arms (for a review, see [8]). Finally, the threading arms repel themselves while the misfit segment becomes longer, and penetrates deeper into the crystal.

In an advanced state (see the thicker line in figure 1) the threading arms are far apart, and a linear misfit segment has developed. The threading arms (screw in nature) do not play

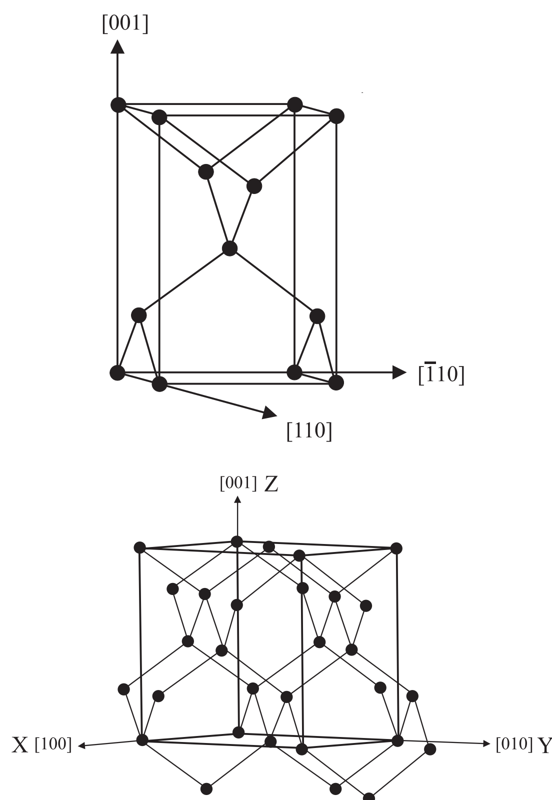

Figure 2. Upper panel: tetrahedral cell used to build our system. Lower panel: conventional cubic cell.

an important role in the strain release process occurring in the close proximity of the misfit segment. Dislocation segments are nucleated in a square network along {110} directions, typically fractions of μm apart for misfit values of 1–2%.

We consider here a $Ge/Si_{0.5}Ge_{0.5}(100)$ system (misfit ∼2%), composed of 63 layers of Ge, each made of 980 atoms, placed over 18 layers of an ordered $Si_{0.5}Ge_{0.5}$ alloy, the two bottom ones frozen to bulk position. The in-plane lattice parameter of the film was set equal to the $Si_{0.5}Ge_{0.5}$ one (size of the conventional cubic cell: 5.542 Å), in order to mimic the typical conditions found in coherent heteroepitaxial structures, i.e. where the film is set to the same lattice parameter of the substrate. The total number of atoms in our simulation cell is 79 380. We made use of a tetrahedral unit cell (see figure 2). Periodic boundary conditions were applied in the [110], [$\bar{1}$10] and [001] directions. With our lattice parameters, the dimensions of the cell are (7.84 nm × 19.2 nm × 14.11 nm). Sufficiently large vacuum was placed over the topmost Ge layer, in order to simulate a free Ge surface. Such a surface was reconstructed in the (100)(2 × 1) configuration.

In order to describe the atomic interactions, we made use of the Tersoff semiempirical potentials [9, 10] which are very good for strain analysis, both in the bulk and at the surface/interface [11]. Due to the long timescales involved, it is impossible to simulate the nucleation process occurring during realistic growth conditions. As a consequence, we used a rough procedure in order to introduce a 60° dislocation in the film: we rigidly deformed the epitaxial layer by reproducing the long-range features, i.e. the displacement field compatible

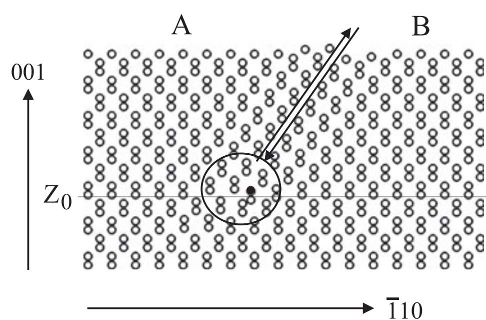

Figure 3. Initial crystal deformation leading to a 60° shuffle dislocation after relaxation. The crystal is represented as projected onto the {110} plane.

to the Burgers vector $\vec{b}$. Subsequently, we relaxed the system, and we verified that the final core geometry corresponds to an actual 60° dislocation (see next section).

We selected the dislocation line to be along the [110] direction, and $\vec{b}$ along the [011] one, initially at an arbitrarily chosen z_0 depth in the Ge layer. The glide plane, defined by the dislocation line and Burgers vector directions, is the $(1\bar{1}1)$ plane starting at z_0. In the shuffle set the glide plane separates two widely distanced {111} planes while in the glide set it divides two closely distanced ones. In the following we shall describe the behaviour of a shuffle misfit segment but the method is still valid in order to reproduce a misfit segment in the glide set [12]. The glide plane divides the crystal into two subregions, indicated as A and B in figure 3. In A, we distorted the crystal by shifting (by ~1 Å), in the direction of $\vec{b}$, the coordinates of the atoms lying in the two double {111} planes closest to the glide plane, with $z > z_0$. Similar displacements were applied to region B, with the only difference being that atoms were shifted in the opposite direction.

The whole procedure is sketched in figure 3, where the system is displayed as projected onto the {110} plane. The arrows represent the atomic displacements. Since the shift is in the [011] direction, there exists also a deformation component in the [110] direction, perpendicular to the plane of the figure. The deformation induces a step at the surface along the [110] direction which is parallel to one of the tetrahedral cell sides. Periodic boundary conditions can thus be safely applied. Notice that such deformation causes the lowering of the atomic density in {001} planes: an atom is missing in each {001} plane above the dislocation line. Above z_0, thus, atoms laying in {001} planes find more space, and they can rearrange themselves increasing the effective lattice parameter.

So far we have described the initial deformation introduced in the film. Starting from such a configuration, we relaxed the simulation cell and we ran several MD simulations.

In our simulations, a time step of 2 fs is used. A standard velocity-rescaling algorithm allowed us to perform simulated annealing runs, and quench the system to the configurational minima. In figure 4 we show in detail the thermal cycle that we have used to study the system evolution, starting from the initial configuration illustrated in figure 3. We increased the temperature from $T = 0$ to 700 K linearly in 30 ps. Subsequently, we ran a long (~0.5 ns) constant-temperature simulation, saving the atomic configurations every 15 ps corresponding to different dislocation positions. All such snapshots were quenched back to 0 K, in order to monitor the actual evolution of the system through different configurational minima. In particular, for each snapshot, the temperature was decreased from 700 to 0 K in 30 ps first, and 20 ps of 0 K simulation finally were run. In the following, we shall describe the configurations relative to a subset of such snapshots, representing different dislocation positions (see cycles (1), (2) and (3) of figure 4).

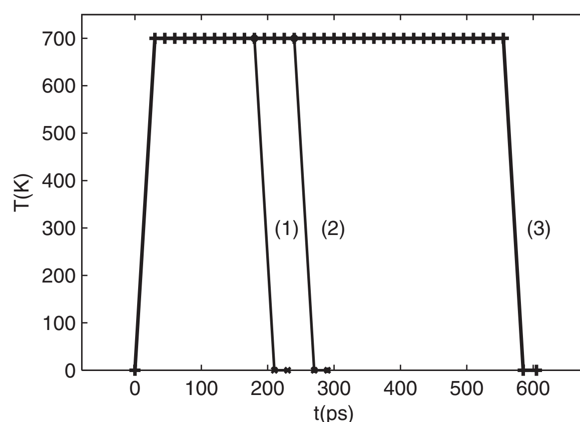

Figure 4. Thermal cycle employed to study the system evolution. Cycle (1) consisted of 30 ps of annealing from 0 to 700 K, 150 ps of MD simulation at 700 K, 30 ps of quenching from 700 to 0 K, and 20 ps of equilibration at 0 K. Cycles (2) and (3) were analogous, except that a longer (210 and 525 ps respectively) MD simulation time at 700 K was considered.

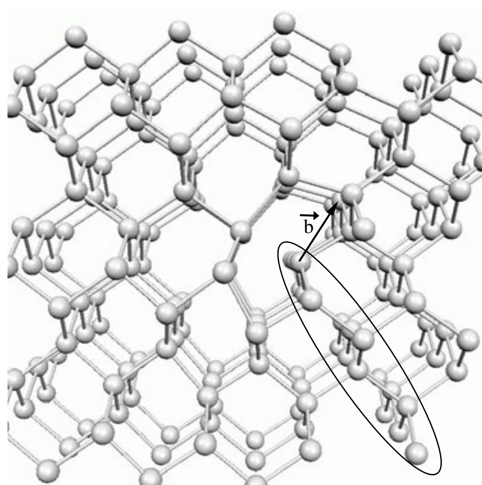

Figure 5. Misfit-segment dislocation core. The additional plane and the dislocation Burgers vector ($\vec{b}$) are indicated.

3. Dislocation geometry and strain maps

As we shall show here below, our procedure allows us to simulate the correct geometry of a 60° shuffle dislocation segment, and the migration of such a segment towards the interface.

Let us start the analysis of our results by looking at the core geometry. Obviously the core geometry does not depend on the dislocation position. In figure 5, for instance, we report the result obtained by performing the thermal cycle (1) of figure 4. The core of the misfit-segment dislocation is shown as projected onto a $\{110\}$ plane. The extra plane is clearly visible (encircled in the figure), and the atomic configuration is exactly correspondent to an ideal 60° shuffle dislocation [13–15].

As is clear from figure 5, atoms close to the dislocation core are highly distorted from the ideal diamond positions. In order to quantify this effect, we have computed detailed

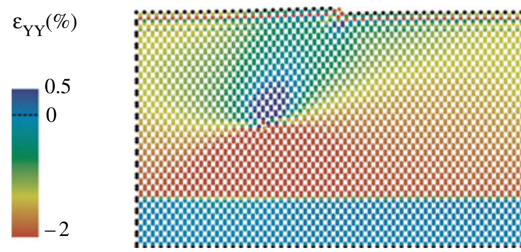

Figure 6. Chromatic map of the ϵ_{YY} component of the strain tensor for a Ge film on a SiGe substrate. Black circles do not represent any particular strain value: they are simply used to display the borders of our cell. The corresponding chromatic scale is reported.

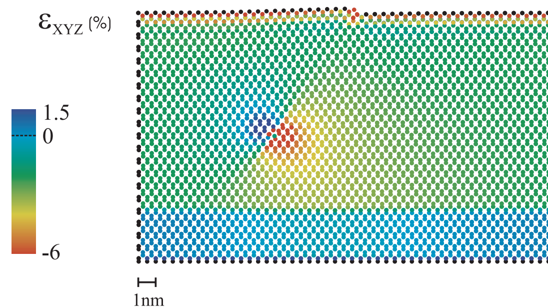

Figure 7. ϵ_{XYZ} strain map.

strain maps. In particular, we have evaluated the strain tensor $\epsilon_{\alpha,\beta}$ at the atomic scale, by considering the transformation matrix between the ideal and the distorted vectors connecting the four nearest neighbours of each atom [16]. In order to present our results concerning strain relaxation, we shall use chromatic maps, where each atom is coloured according to its strain. Let us first analyse the strain maps relative to the configuration obtained after performing the cycle (2) of figure 4. In this configuration the dislocation is close to the centre of the Ge layer. The maps are reported in figures 6 and 7, where the crystal is projected as in figure 3. Due to the particular orientation of $\vec{b}$ ([011]), the deformation induced by the dislocation has its strongest components in the [001] and [010] directions. Therefore, we have computed the strain tensor with respect to the conventional cubic cell (see the lower panel of figure 2), so that ϵ_{YY} will indicate the diagonal component of the strain tensor along the [010] direction, and ϵ_{ZZ} the corresponding one in the [001] direction. As a consequence, the most significant component of the strain tensor is the ϵ_{YY} one, describing the in-plane lattice relaxation due to the dislocation. Strain is computed with respect to the ideal lattice parameter of the local composition, i.e. to the bulk $Si_{0.5}Ge_{0.5}$ parameter for the substrate and to the bulk Ge parameter for the epilayer.

In figure 6 the ϵ_{YY} component is represented. The dislocation line is perpendicular to the figure. The free Ge surface is located at the top of the figure while the SiGe substrate is at the bottom. The chromatic scale boundaries are chosen in order to facilitate the understanding of the main elastic features in the whole system. In particular, red indicates a $\sim$2% compressive strain, light blue an absence of strain, while dark blue indicates a small ($\sim$0.5%) expansion. As expected, we note that the atoms which are located below the dislocation core (which lies at the boundary between the dark blue region and the red region) are coloured in red, meaning that the strain remains at a $\sim$2% value, typical of the pseudomorphic epilayer. One can easily

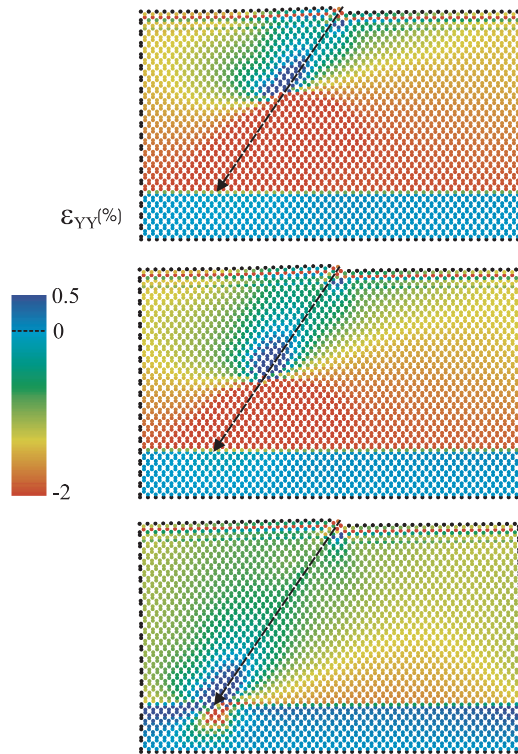

Figure 8. Evolution of the ϵ_{YY} strain component during the dislocation motion towards the interface. The black arrow indicates the motion direction which occurs along the glide plane.

individualize a small blue region surrounding the dislocation core. Inside this region, Ge atoms are slightly expanded in the Y direction with respect to the pure Ge lattice parameter. Above the dislocation, atoms appear coloured in green and yellow, meaning that they are partially relaxed. A direct calculation of the average residual strain in such a region yields $\sim$1%.

The reason why relaxation is not complete (only 1%) is easily understood. The $\vec{b}$ component in the Y direction is given by $a/2$, where a is the $Si_{0.5}Ge_{0.5}$ lattice parameter. With our simulation cell, taking into account periodic boundary conditions, this additional space is distributed among a total length of $49a$, thus allowing the system to relax by only $\sim$1%. In order to relax the whole 2% lattice mismatch, one should use a much smaller simulation cell. However, in doing so, due to periodic boundary conditions, the lateral interactions between adjacent dislocations would become very important, possibly dominating the whole strain-release process. In real systems, dislocations nucleate randomly at different depths, and, at least at a first stage, they can be considered as isolated.

In the strain map discussed above, the chromatic scale was set in order to explore the medium- and long-range elastic effects linked to the presence of the dislocation. However, an extended scale allows us to reveal interesting short-range effects in the close proximity of the dislocation core. In figure 7 we report the hydrostatic strain $\epsilon_{XYZ} = \epsilon_{XX} + \epsilon_{YY} + \epsilon_{ZZ}$, on a different scale. The analysis of ϵ_{hy} is of particular interest since its value gives an indication of the average volume distortion. As appears clearly in the figure, the presence of the misfit-segment dislocation causes the formation of two lobes (red and blue regions), symmetrically

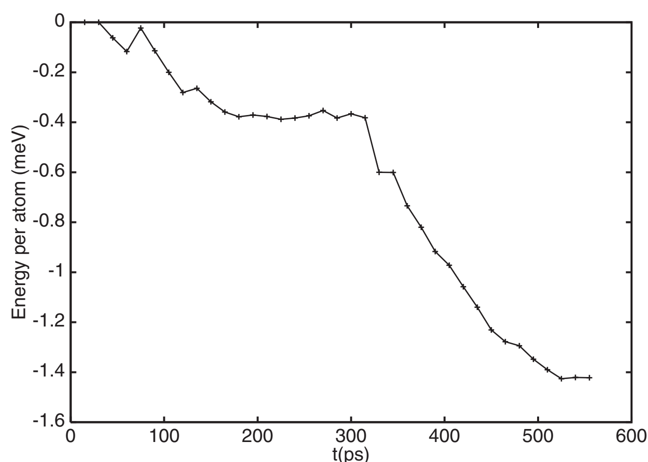

Figure 9. Total energy of the system (per atom) versus simulation time. After ~500 ps, the dislocation reaches the Ge/SiGe interface. To compute the energy, every simulation snapshot was quenched to 0 K. The energy of the initial configuration is used as a reference.

positioned with respect to the glide plane, with a strong strain gradient. One of them, positioned at the left of the glide plane in the figure, represents a tensile-strain region, the other one a compressive-strain one where an additional atomic layer is present (see figure 5). However, both the compressed lobe and the expanded one have a linear extension of a few nanometres. This elastic field feature has been already reported for $Si_{0.5}Ge_{0.5}/Si(001)$ films in [17], where consequent SiGe dealloying in the close proximity of the dislocation core was suggested.

In the next section we shall describe the main issue of the work: the migration of the dislocation segment monitored at the atomic scale by MD simulations.

4. Migration towards the interface

As we have already pointed out, after nucleation the misfit segment tends to migrate towards the interface, thus releasing the strain in the film. In our simulations we observe this process directly. In figure 8 the evolution of the ϵ_{YY} component of the strain tensor in the whole simulation is represented. The chromatic scale is the same as that used in figure 6. In the upper panel (representing the quenched configuration relative to the thermal cycle (1) of figure 4) the dislocation is still close to the free surface. As a consequence, strain release occurs in a very limited part of the crystal, as is demonstrated by the wide red region below it. By proceeding with the annealing time, the core moves downwards (central panel, thermal cycle (2)), along the glide plane, until it reaches the interface (lower panel, thermal cycle (3)). At this point, the whole epilayer is relaxed and appears coloured in green (we recall once again that the system still contains a ~1% residual strain). It is interesting to note that, as soon as the $Si_{0.5}Ge_{0.5}$ interface is reached by the core, a small compressive region is formed in the $Si_{0.5}Ge_{0.5}$ substrate.

The energy gain per atom during the whole process is displayed in figure 9, as a function of the simulation time. The reference energy is set to the one corresponding to the first relaxed configuration in the thermal cycle of figure 4. Time is taken from the instant where such a configuration is obtained. Actually, the process includes both the lowering of a small segment of the dislocation line and kink propagations along the latter.

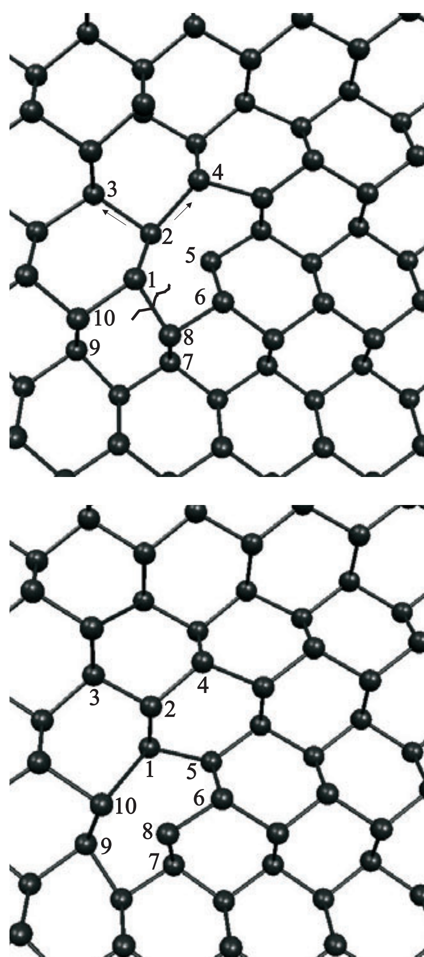

Figure 10. Dislocation core evolution between two successive configurations. Atom numbering is the same.

The local migration of a small segment involves several atoms. A close inspection of a series of snapshots recorded during the simulation allows us to capture the basic microscopic processes underlying such motion. In a simplified view, the diffusion mechanism at the atomic level turns out to be the one represented in figure 10. In moving from the upper panel to the lower panel of the figure, the dislocation moves towards the SiGe interface by a double atomic layer. On the plane perpendicular to the dislocation line, 10 atoms are mainly involved in the mechanism. Atoms 1 and 2 act as a dimer, and make a concerted move involving a broken bond (displayed by the wiggle in the upper panel of the figure), a rotation and a translation, which leads to the formation of a new bonds (1–5 bond in the lower panel of the figure). Such motion also implies a significant stretch of further bonds, such as the 9–10 and the 1–10 ones. The extra plane glides down by a double plane: atoms 7 and 8 in the lower panel, while, in order to complete the perfect core structure, the 9–10 dimer (lower) replaces the 1–2 dimer (upper).

So far we have discussed the behaviour of the atoms in a small segment of the dislocation line. The migration of the whole misfit dislocation segment can be described as a nucleation process and a lateral motion of kinks along the dislocation line [14]. Unfortunately, we could

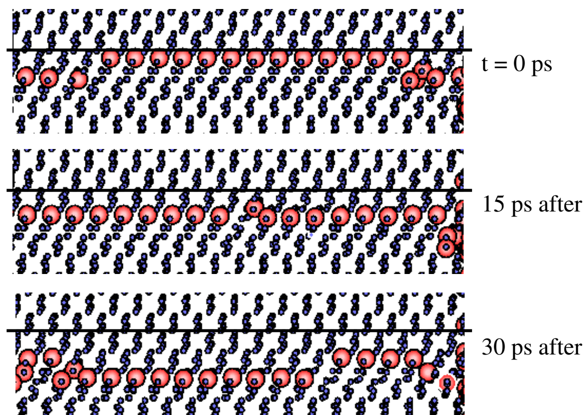

Figure 11. Three stages of the dislocation motion towards the interface in a crystal section along the dislocation line. In the first panel two kinks are evident. The segment between them glides down in the second panel. In the following stage another kink pair is developed. The black line is used as reference.

not resolve the lateral motion of the kinks at the atomic scale. In fact when we observed the dislocation line during the high-temperature simulation run, the thermal noise was predominant and kinks were not unambiguously identified. More information could be obtained by observing the evolution of the dislocation line from a lateral view in a series of quenched snapshots (i.e. every 15 ps during the motion). For example, in figure 11 three subsequent quenched snapshots are reported. The red large circles represent the undercoordinated core atoms along the dislocation line (atoms 5 or 8 in the core structure following the numbering in figure 10). Two kinks are present in the first stage, then all the central part of the dislocation line reaches the double layer below and in the third step again two kinks nucleate and a segment goes further down towards the interface.

5. Conclusions

In this paper we have presented an atomistic study of a shuffle 60° dislocation moving in a $Ge/Si_{0.5}Ge_{0.5}(100)$ system towards the interface. We initially inserted the misfit segment in the film by a suitable rigid displacement of the lattice, and evolved the system by molecular dynamics simulations at 700 K. In particular, we followed the progressive strain release in the whole film during the motion while observing the underlying elementary atomic-scale mechanisms. We have individuated the microscopic kinks created at the dislocation line and we have shown that, within a small portion of the line which is coherently moving, the elementary atomic motion leading to dislocation gliding can be easily tracked.

References

[1] Mooney P M and Chu J O 2000 *Annu. Rev. Mater. Res.* **30** 335
[2] Fitzgerald E A, Xie Y H, Green M L, Brasen D, Kortan A R, Michel J, Miim Y J and Weir B E 1991 *Appl. Phys. Lett.* **59** 811
[3] Matthews J W and Blakeslee A E 1974 *J. Cryst. Growth* **27** 118
[4] Miglio L and Sassella A 2005 *Encyclopedia of Condensed Matter Physics* ed G F Bassani, G L Liedl and P Wyder (Amsterdam: Elsevier–Academic)

[5] von Känel H, Onida N and Miglio L 1995 *Science and Technology of Thin Films* ed G P Ottaviani and C M Mattacotta (Singapore: World Scientific)
[6] Tsao J Y 1997 *Materials Fundamentals of Molecular Beam Epitaxy* (Albuquerque, NM: Academic)
[7] Marian J, Cai W and Bulatov V V 2004 *Nat. Mater.* **3** 158
[8] Fitzgerald E A 1995 *Annu. Rev. Mater. Sci.* **25** 417
[9] Tersoff J 1988 *Phys. Rev.* B **37** 6991
[10] Tersoff J 1989 *Phys. Rev.* B **39** 5566
[11] Raiteri P, Miglio L, Valentinotti F and Celino M 2002 *Appl. Phys. Lett.* **80** 3736
[12] Marzegalli A, Montalenti F and Miglio L 2005 *Appl. Phys. Lett.* **86** 041912
[13] Hornstra J 1958 *J. Phys. Chem. Solids* **5** 129
[14] Hirth J P and Lothe J 1992 *Theory of Dislocations* (Malabar, FL: Krieger)
[15] Claeys C and Vanhellemont J 1994 *Advanced Silicon and Semiconducting Silicon-Alloy Based Materials and Devices* (Bristol: JFANijs)
[16] Pryor C, Kim J, Wang L W, Williamson A J and Zunger A 1998 *J. Appl. Phys.* **83** 2548
[17] Martinelli L, Marzegalli A, Raiteri P, Bollani M, Montalenti F, Miglio L, Chrastina D, Isella G and von Känel H 2004 *Appl. Phys. Lett.* **84** 2895